

# Impact Sintering Temperatures on Mechanical Properties of Ba<sub>1-x</sub>Sr<sub>x</sub>TiO<sub>3</sub>

Hamed A. Gatea<sup>1,\*</sup> and Mohammed Ayad Alkhafaji<sup>2</sup>

<sup>1</sup>Department of Medical Physics, College of Applied Medical Science, Shatrah University, Thi-Qar, 64001, Iraq

<sup>2</sup>Department of Medical Device, Collage of Pharmacy, National University of Science and Technology, Dhi Qar, 64001, Iraq

Received: 12 Nov. 2024, Revised: 12 Dec. 2024, Accepted: 23 Dec. 2024

Published online: 1 Jan. 2025

**Abstract:** This study investigates the influence of sintering temperatures on the mechanical properties of Ba<sub>1-x</sub>Sr<sub>x</sub>TiO<sub>3</sub> ceramics. Ba<sub>1-x</sub>Sr<sub>x</sub>TiO<sub>3</sub>(x=0.2) ceramics are synthesized via Sol-Gel and sintered at varying temperatures. We use the appropriate testing methods to describe mechanical qualities like hardness, fracture toughness, and elastic modulus. The results show that the mechanical behavior changes a lot when the sintering temperature changes. This shows how important processing conditions are for customizing the mechanical performance of Ba<sub>1-x</sub>Sr<sub>x</sub>TiO<sub>3</sub> ceramics that could be used in advanced electronic and structural materials. XRD pattern exhibited a tetragonal phase, and the crystal size increased with increasing sintering temperature. The BST sample's surface morphology appears uniform and homogeneous, with moderate sintering temperatures. High Sintering Temperature, and higher density as the material achieves better grain growth and packing, reducing porosity. High Sintering Temperature increases mechanical strength due to improved densification and reduced porosity, producing higher hardness because of increased density and larger, well-formed grains and improved fracture toughness as the material becomes denser and grain boundaries are better formed, enhancing crack resistance. Also, (c/a ratio) was found to decrease with an increase in sintering temperatures.

**Keywords:** Ba<sub>1-x</sub>Sr<sub>x</sub>TiO<sub>3</sub>, Mechanical Properties, Sintering Temperatures, hardness, toughness.

## 1 Introduction

Ba<sub>1-x</sub>Sr<sub>x</sub>TiO<sub>3</sub> ceramics have received considerable interest due to their varied uses in electronic devices, capacitors, and structural materials because of their remarkable dielectric and ferroelectric properties [1][2][3]. A comprehensive comprehension of the impact of manufacturing parameters, such as the sintering temperature, on the mechanical behavior of these ceramics is essential for their functionality in a variety of applications [4][5][6]. The sintering temperature is an important factor in ceramic processing because it affects the growth of grains, the development of microstructures, and the formation of defects [7][6]. These changes have a direct effect on mechanical traits like hardness, fracture toughness, and elastic modulus [8][9].

Ba<sub>1-x</sub>Sr<sub>x</sub>TiO<sub>3</sub> (BST) compounds, which are part of the perovskite family, have a diverse range of uses in different disciplines because of their outstanding dielectric and ferroelectric properties [10]. The composition and processing conditions, particularly the sintering temperature, significantly influence the tuning of these properties [11][12]. Among the primary elements determining these qualities, sintering temperature stands out as a critical parameter controlling the microstructure and, as a result, the material's mechanical behavior [13][14].

This study examines the influence of sintering temperatures

ranging from 1000°C to 1400°C on the mechanical characteristics of BST ceramics. The primary objective is to analyze how different sintering temperatures affect the mechanical properties of BST ceramics. Understanding these relationships is essential for optimizing the material's performance in practical applications. This research aims to provide insights into how variations in sintering temperature affect the mechanical characteristics of BST ceramics, thereby contributing to the broader understanding and enhancement of their functional properties [15]. Understanding how variations in sintering temperature influence the mechanical performance of BST ceramics is essential for optimizing their structural integrity and reliability in practical applications [16][17].

This work aims to understand thoroughly the effects of sintering conditions and mechanical properties (such as elastic modulus, attenuation, and velocity of ultrasonic waves) of Ba<sub>(1-x)</sub>Sr<sub>(x)</sub>TiO<sub>3</sub> ceramics sintered at 1000 to 1400°C for 3h. X-ray diffraction and ultrasonic techniques (at a frequency of 2 MHz) were used to characterize the structure and phase transitions of the prepared BST ceramics.

## 2. Experimental procedures

Ba<sub>0.8</sub>Sr<sub>0.2</sub>TiO<sub>3</sub> ceramics were prepared by the new method called the sol-gel method. The Barium acetate, strontium acetate, and Ti isopropoxide (IV) were mixed in the appropriate molar ratios (1:1). First, the Ba and Sr acetate solution was mixed and stirred at 60°C. Second, the Ti isopropoxide with 2-

\*Corresponding author E-mail: [hamedalwan14@gmail.com](mailto:hamedalwan14@gmail.com)

methanol was mixed and added to the first solution. The mixture solution was calcined at 700°C for 3 h in open air. The produced fine powders were pressed into disc-shaped pellets (D:10 mm and Th: 2 mm) at an isostatic pressure of 12 tons. The pelletized samples were sintered at different sintering temperatures.

### Characterization:

“X-ray powder diffraction (XRD) was conducted using Cu Ka ( $k = 1.54056 \text{ \AA}$ ) radiation at 40 kV and 40 mA. The microstructure was visualized using scanning electron microscopy (FESEM, JSM EMP-800, JEOL, Japan) [12]. The ultrasonic wave velocities  $v$  (in  $\text{ms}^{-1}$ ) propagated in the samples and attenuation  $\alpha$  (dB/cm) were measured at room temperature, using pulse-echo technique MATEC Model MBS8000 DSP (ultrasonic digital signal processing) system with 2 MHz resonating.

## 3. Results and Discussion

Finding the sweet spot for BaSrTiO<sub>3</sub> sintering temperature involves juggling densification, grain development, and optimizing mechanical properties. When the temperature is too high, it can cause grain growth and compromise mechanical qualities; when the temperature is too low, densification is inadequate. Ultimately, the sintering temperature is crucial in establishing the mechanical characteristics of BaSrTiO<sub>3</sub> as shown in Fig. 1. By manipulating the sintering temperature, it is possible to customize the density, grain size, hardness, fracture toughness, dielectric characteristics, and mechanical strength of the material to fulfill specific application demands. The densification factor exhibited a positive correlation with temperature, increasing until it reached its maximum concentration. A positive densification factor indicates that ceramics shrink during the sintering process.

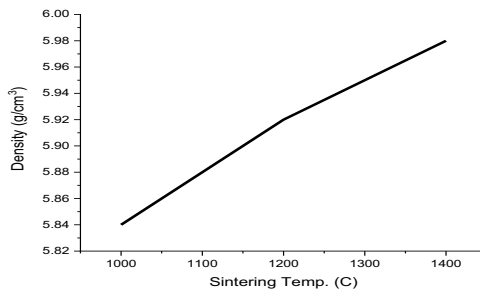


Fig. 1: The sintering temperature vs density of Ba<sub>0.8</sub>Sr<sub>0.2</sub>TiO<sub>3</sub>

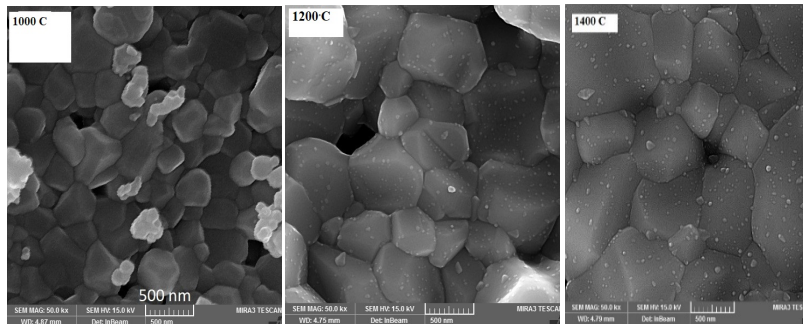


Fig. 2: Images of FESEM for surface morphology Ba<sub>0.8</sub>Sr<sub>0.2</sub>TiO<sub>2</sub>

The density of BaSrTiO<sub>3</sub> (barium strontium titanate) is strongly influenced by sintering temperature. Generally, as the sintering temperature increases, the density of the material also increases. This relationship is due to the processes of densification and grain growth that occur during sintering.

$$DF = \frac{\rho_m - \rho_g}{\rho_t - \rho_g} \quad (1)$$

“Where  $\rho_g$  represented the density of green pellets,  $\rho_t$  theoretical density and  $\rho_m$  is the measured density”

The shrinking measurement checked the diameters of both pre-sintering samples

$$D_{shrinking} = \frac{d_o - d_s}{d_o} \quad (2)$$

“Where  $d_o$  and  $d_s$  are the diameter of the green and sintered pellets, respectively”

## 4. Microstructural Evolution

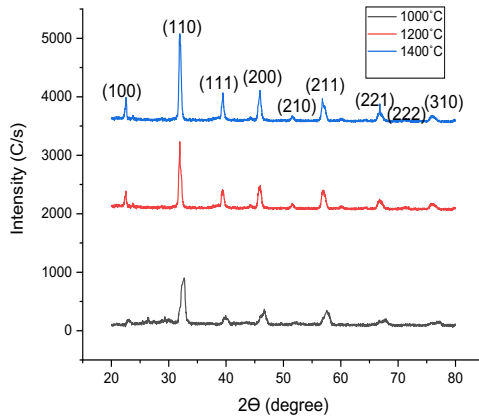
### 4.1 Morphology and Surface Characteristics

Fig. 2 displays the FESEM picture of the BaTiO<sub>3</sub> ceramic system at various sintering temperatures. The BaTiO<sub>3</sub> ceramic, heated to 1150 °C, exhibits an open structure due to the loose packing of particles. This makes the ceramic less dense. At a temperature of 1200 °C, the particles start to form bonds, but the density of pores remains high. At a temperature of 1250 °C, the particles coalesced, and no empty spaces were detected. Nevertheless, the surface microstructure and the particle boundaries remain ambiguous. At a sintering temperature of 1300 °C, the pores are nearly eliminated, resulting in a strongly bonded grain boundary and the formation of a high-density ceramic.

As the temperature continues to rise until it reaches 1400 °C, the grain size increases, and holes appear around the edge and inside the seed. The morphology and surface features of the material significantly determine the mechanical properties of Ba<sub>0.8</sub>Sr<sub>0.2</sub>TiO<sub>3</sub> (BST) ceramics. Differences in the temperature during the sintering process control these qualities. Field emission scanning electron microscopy (FESEM) pictures showed that the sintering temperature had a big effect on the size and spread of the grains. Lower sintering temperatures, between 1000°C and 1200°C, resulted in smaller and more evenly distributed grains in BST ceramics (Fig. 2). As the temperature of the sintering rose to 1400 °C, grain growth was seen.

### 4.2 Phase Composition

X-ray diffraction (XRD) analysis validated the phase purity and crystallinity of BST ceramics across various sintering temperatures. There were unique peaks that corresponded to the creation of specific phases, such as tetragonal and cubic phases, at different sintering temperatures (Fig. 3) Illustration. Ceramics with Ba<sub>1-x</sub>Sr<sub>x</sub>TiO<sub>3</sub> (x=0.2) X-ray diffraction patterns Fig. 3 depicts the indexing of all the peaks. These indices relate to the reflections of the various polycrystalline orientations, with the 110 indices being the high-intensity main peak. It shows that as the sintering temperatures increased from 1000 to 1400°C, the peak positions at 2θ° angles 31.83251°, 31.88799°, and 32.06737° were confirmed by a closer examination of the 110 peaks for all samples. Scherrer's equation is used to estimate the crystallite size D (hkl) by referring to the broadening of the x-ray line's half-width. The table below lists the evolution of crystal structure, lattice parameters, and crystallite size obtained from XRD data. Table 1 shows that increasing the sintering temperatures leads to an increase in both lattice parameters and crystallite size. The crystal structure showed tetragonal phases for all tested samples and the tetragonality ratio (c/a) decreased as the sintering temperature increased as reported [12].



**Fig. 3:** XRD pattern for Ba<sub>0.8</sub>Sr<sub>0.2</sub>TiO<sub>3</sub> with different sintering temperatures

**Table 1:** The sintering temperatures vs lattice parameters, crystallite size and Tetragonality

Sintering Temp. C	a (Å)	c (Å)	Phase	The Tetragonality ratio (c/a)	Volume(Å <sup>3</sup> )	D (nm)
1000	3.9771	3.9885	Tetragonal	1.0038	64.08	22.78
1200	3.97815	3.9922	Tetragonal	1.003531	63.89	32.11
1400	3.97872	3.9941	Tetragonal	1.00286	63.82	36.60

## 5. Mechanical Properties

Indentation tests revealed variations in the hardness and fracture toughness of BST ceramics as a function of sintering temperature. Generally, higher sintering

temperatures led to increased hardness due to improved densification and grain growth, whereas fracture toughness showed a more complex relationship influenced by microstructural features (Fig. 5). The ultrasonic wave velocities *v* were calculated by taking the elapsed time between the initiation and the receipt of the pulse appearing on the screen. It can be calculated using the following equation:

$$v = \frac{2x}{\Delta t} \tag{3}$$

“Where *x* is the sample thickness and  $\Delta t$  is the time interval. The measurements were repeated three times to check the reproducibility of the data. The estimated accuracy of the velocity measurement is about 0.04%. The values of elastic moduli; namely longitudinal modulus (L), shear modulus (G), Young's modulus (E), bulk modulus (B), and Poisson's ratio ( $\sigma$ ) were obtained from the longitudinal (VL)<sup>2</sup> and shear (VS)<sup>2</sup> ultrasonic velocities and calculated from the following equations:”[7]

$$L = \rho v_L^2 \tag{4}$$

$$G = \rho v_S^2 \tag{5}$$

$$E = \frac{G(3L-4G)}{(L-G)} \tag{6}$$

**Table 2:** The sintering temperatures vs the mechanical properties (L, G, and E), particle size

Sintering Temp. °C	Density (Kg/m <sup>3</sup> )	Long. Velocity V <sub>L</sub> (m/s)	Elastic Modulus L(GPa)	longitudinal modulus (L)	shear modulus (G)	Particles size(nm)
1000	5.83	634.56	4.17	7.56	2.22	78.71
1200	5.89	1178.89	11.45	14.78	4.67	132.11
1400	5.93	1278.57	16.34	18.98	6.98	141.60

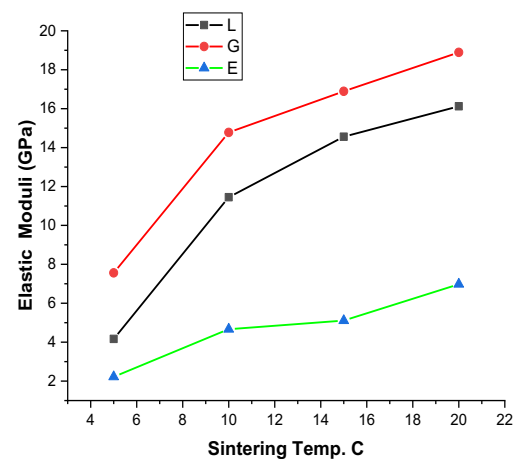


**Fig. 4:** Elastic Moduli E, G, L vs sintering temperatures

Effects of Sintering Temperature An increase in the sintering temperature can cause changes in the material's

microstructure, including changes in grain size and porosity. In general, greater sintering temperatures tend to decrease porosity and increase grain size, which ultimately leads to an increase in the longitudinal modulus. Increased density and uniformity in a structure typically lead to increased stiffness in the direction of the applied force. Longitudinal Modulus (L): Increases with higher sintering temperature due to reduced porosity and increased grain size. Shear Modulus (G): Increases with higher sintering temperature as the material becomes denser and more homogeneous. Young's Modulus (E): Typically increases with higher sintering temperature due to improved structural integrity and stiffness. Bulk Modulus (B): Increases with higher sintering temperature as the material becomes more dense and less compressible.

## 6. Conclusion

The observed changes in morphology and surface characteristics underscore the intricate relationship between processing parameters (sintering temperature) and the microstructural evolution of BST ceramics. Higher temperatures significantly impact mechanical properties such as hardness, fracture toughness, and flexural strength. Understanding these relationships is crucial for tailoring BST ceramics with optimized mechanical performance for diverse applications in electronics, telecommunications, and beyond. Overall, the results highlight the importance of precise control over sintering parameters to achieve desired microstructural features and mechanical properties in  $Ba_{1-x}Sr_xTiO_3$  ceramics, paving the way for further advancements in materials design and application-specific optimizations. This structured approach integrates both results and discussion, emphasizing the interplay between sintering temperature and mechanical properties of BST ceramics.

## Acknowledgments

We would like to thank everyone who helped the authors finish this study.

## Conflict of Interest

The project has no financing, and the authors have declared no competing financial interests.

## Availability of data materials

We won't disclose the data because it helps with the study of choosing the right forms for the right applications.

## References:

- [1] H. A. Gatea, S. J. Shoja, and H. J. Albazoni, "Effect of Sr<sup>+2</sup> Substitution on the Structural and Optical Properties of  $Ba_{1-x}Sr_xTiO_3$ ," *Jom*, vol. 75, no. 11, pp. 4470–4478, 2023, doi: 10.1007/s11837-023-06052-6.
- [2] H. A. Gatea, H. Abbas, and M. L. Shaghnab, "Impact of High Heat Treatment on Ferroelectric Materials Properties:  $Ba_{1-x}Sr_xTiO_3$  as a Model," *ECS J. Solid State Sci. Technol.*, vol. 12, no. 8, p. 083002, Aug. 2023, doi: 10.1149/2162-8777/acec11.
- [3] D. J. K. Myang Hwan Lee, Hae In Choi, "Ferroelectric Polarization Dependent Piezoelectric Hardening in  $BiFeO_3$ - $BaTiO_3$  Lead-Free Ceramics," *Adv. Electron. Mater.*, vol. 7, no. 1, p. 2300902, 2024.
- [4] V. R. N. A and Christian Maier, "Synergistic homovalent and heterovalent substitution effects on piezoelectric and relaxor behavior in lead-free  $BaTiO_3$  ceramics," *J. Eur. Ceram. Soc.*, vol. 44, p. 116689, 2024.
- [5] H. A. Gatea, H. Abbas, and I. S. Naaji, "Effect of Sr<sup>+</sup> ion Concentration on Microstructure and Dielectric properties of Barium Strontium Titanate Ceramics," *Int. J. Thin Film Sci. Technol.*, vol. 11, no. 2, 2022, doi: 10.18576/ijtfst/110212.
- [6] H. A. Gatea, "Effect of substrate-induced strains on ferroelectric and dielectric properties of lead zirconate titanate films prepared by the sol-gel technique," *Nanosci. Nanotechnol. - Asia*, vol. 11, no. 3, 2021, doi: 10.2174/2210681210999200715105250.
- [7] H. A. Gatea and S. M. Khalil, "Evaluating the impact of substrate deposition on optical properties of perovskite barium strontium titanate ( $Ba_{0.5}Sr_{0.5}TiO_3$ ) thin films prepared by pulsed laser deposition technique," *Eur. Phys. J. D*, vol. 76, no. 8, 2022, doi: 10.1140/epjd/s10053-022-00462-y.
- [8] M. Misra, K. Kotani, T. Kiwa, I. Kawayama, H. Murakami, and M. Tonouchi, "THz time domain spectroscopy of pulsed laser deposited  $BaTiO_3$  thin films," *Appl. Surf. Sci.*, vol. 237, no. 1–4, pp. 421–426, 2004, doi: 10.1016/j.apsusc.2004.06.062.
- [9] C. J. Huang, K. Li, S. Y. Wu, X. L. Zhu, and X. M. Chen, "ScienceDirect Variation of ferroelectric hysteresis loop with temperature in ( $Sr_xBa_{1-x}$ )  $Nb_2O_6$  unfilled tungsten bronze ceramics," *J. Mater.*, vol. 2, pp. 2–7, 2015, doi: 10.1016/j.jmat.2015.02.004.
- [10] X. Wang, P. Bao, and T. J. J. M. J. Lancaster, "Tunable microwave filters based on discrete ferroelectric and semiconductor varactors," *IET Microw. Antennas Propag.*, vol. 5, no. 7, pp. 776–782, 2011, doi: 10.1049/iet-map.2010.0417.
- [11] D. Sitko and W. Piekarczyk, "Phase Transitions: A Multinational Composition-related structural, thermal and mechanical properties of," no. June, pp. 37–41, 2015, doi: 10.1080/01411594.2015.1020310.
- [12] N. Novizal, A. Manaf, and P. Sardjono, "Crystallite size characterization of mechanically alloyed of

- (Ba,Sr) hexaferrite and (Ba,Sr) titanate composite system,” *Adv. Mater. Res.*, vol. 789, pp. 76–81, 2013, doi: 10.4028/www.scientific.net/AMR.789.76.
- [13] Rusiyanto *et al.*, “Effect of Sintering Temperature on the Physical Properties of Ba<sub>0.6</sub>Sr<sub>0.4</sub>TiO<sub>3</sub> Prepared by Solid-State Reaction,” *Int. J. Automot. Mech. Eng.*, vol. 18, no. 2, pp. 8752–8759, 2021, doi: 10.15282/ijame.18.2.2021.13.0669.
- [14] Hamed A. Gatea and Sarah M., “Comparative study of the dielectric properties of the bulk and film of perovskite Ba<sub>0.6</sub>Sr<sub>0.4</sub>TiO<sub>3</sub>,” *Int. J. Mod. Phys. B*, 2023.
- [15] H. A. Gatea, “Synthesis and characterization of basrti03 perovskite thin films prepared by sol gel technique,” *Int. J. Thin Film Sci. Technol.*, vol. 10, no. 2, pp. 95–100, 2021, doi: 10.18576/ijfst/100204.
- [16] P. van Assenbergh, E. Meinders, J. Geraedts, and D. Dodou, “Nanostructure and Microstructure Fabrication: From Desired Properties to Suitable Processes,” *Small*, vol. 14, no. 20, pp. 1–24, 2018, doi: 10.1002/smll.201703401.
- [17] C. A. Secondary, C. Author, I. Naji, and A. Abulameer, “Photonic Sensors Humidity sensing properties of ferroelectric compound Ba<sub>0.7</sub>Sr<sub>0.3</sub>TiO<sub>3</sub> thin films grown by pulsed laser deposition”.